

Alma Mater Studiorum Università di Bologna  
Archivio istituzionale della ricerca

Bio-based and one-day compostable poly(diethylene 2,5-furanoate) for sustainable flexible food packaging:  
Effect of ether-oxygen atom insertion on the final properties

This is the final peer-reviewed author's accepted manuscript (postprint) of the following publication:

*Published Version:*

Quattrosoldi S., Guidotti G., Soccio M., Siracusa V., Lotti N. (2022). Bio-based and one-day compostable poly(diethylene 2,5-furanoate) for sustainable flexible food packaging: Effect of ether-oxygen atom insertion on the final properties. CHEMOSPHERE, 291(Part 2), 1-11 [10.1016/j.chemosphere.2021.132996].

*Availability:*

This version is available at: <https://hdl.handle.net/11585/852086> since: 2022-02-21

*Published:*

DOI: <http://doi.org/10.1016/j.chemosphere.2021.132996>

*Terms of use:*

Some rights reserved. The terms and conditions for the reuse of this version of the manuscript are specified in the publishing policy. For all terms of use and more information see the publisher's website.

This item was downloaded from IRIS Università di Bologna (<https://cris.unibo.it/>).  
When citing, please refer to the published version.

(Article begins on next page)

**Bio-based and one-day compostable poly(diethylene 2,5-furanoate) for sustainable flexible food packaging: effect of ether-oxygen atom insertion on the final properties**

*Silvia Quattrosoldi <sup>a§</sup>, Giulia Guidotti <sup>a§</sup>, Michelina Soccio <sup>a,c\*</sup>, Valentina Siracusa <sup>b</sup>, Nadia Lotti <sup>a,c,d</sup>*

<sup>a</sup>Civil, Chemical, Environmental and Materials Engineering Department, University of Bologna,

Via Terracini 28, 40131 Bologna, Italy

<sup>b</sup>Chemical Science Department, University of Catania, Viale A. Doria 6, 95125 Catania, Italy

<sup>c</sup>Interdepartmental Center for Industrial Research on Advanced Applications in Mechanical Engineering and Materials Technology, CIRI-MAM, University of Bologna, Bologna, Italy

<sup>d</sup> Interdepartmental Center for Agro-Food Research, CIRI-AGRO, University of Bologna, Bologna, Italy.

**Keywords:** 2,5-furandicarboxylic acid; ether linkage; barrier properties; mechanical properties; compostability

§ These authors contributed equally.

## 22    **Abstract**

23    In the present work, the effect of ether oxygen atom introduction in a furan ring-containing polymer  
24    has been evaluated. Solvent-free polycondensation process permitted the preparation of high  
25    molecular weight poly(diethylene 2,5-furandicarboxylate) (PDEF), by reacting the dimethyl ester of  
26    2,5-furandicarboxylic acid with diethylene glycol. After molecular and thermal characterization,  
27    PDEF mechanical response and gas barrier properties to O<sub>2</sub> and CO<sub>2</sub>, measured at different  
28    temperatures and humidity, were studied and compared with those of poly(butylene 2,5-  
29    furandicarboxylate) (PBF) and poly(pentamethylene 2,5-furanoate) (PPeF) previously determined.  
30    Both PDEF and PPeF films were amorphous, differently from PBF one. Glass transition temperature  
31    of PDEF (24 °C) is between those of PBF (39 °C) and PPeF (13 °C). As concerns mechanical  
32    response, PDEF is more flexible (elastic modulus [E] = 673 MPa) than PBF (E = 1290 MPa) but stiffer  
33    than PPeF (E = 9 MPa). Moreover, PDEF is the most thermally stable (temperature of maximum  
34    degradation rate being 418 for PDEF, 407 for PBF and 414 °C for PPeF) and hydrophilic (water  
35    contact angle being 74 ° for PDEF, 90 ° for PBF and 93 ° for PPeF), with gas barrier performances  
36    very similar to those of PPeF (O<sub>2</sub> and CO<sub>2</sub> transmission rate being 0.0022 and 0.0018 for PDEF and,  
37    0.0016 and 0.0014 cm<sup>3</sup> cm / m<sup>2</sup> d atm for PPeF). Lab scale composting experiments indicated that  
38    PDEF and PPeF were compostable, the former degrading faster, in just one day.  
39    The results obtained are explained on the basis of the high electronegativity of ether oxygen atom  
40    with respect to the carbon one, and the consequent increase of dipoles along the macromolecule.

41

## 1. Introduction

Although relatively new compared to wood, glass and metals, these last used by man since the dawn of time, plastics have been used more and more and today they are practically irreplaceable. As proof of this, their production has increased from 270 million metric tons to almost 370 million metric tons from 2010 to 2020, and it is expected to further increase, rising to about 590 million metric tons by 2050.<sup>1,2</sup> Their global market is also expected to reach 750.1 billion of dollars by 2028.<sup>3</sup> Such a massive use of plastics entails a significant impact on both exploitation of non-renewable sources and on accumulation of wastes in the marine and terrestrial habitats. The environmental problems caused by human activity are one of the main themes of debate of the last Century. With the perspective of reducing the environmental issues and building a new circular economy, the employment of renewable resources for plastic production and plastic waste recycling are the most suitable solutions. For this reason, sustainable materials are attracting a continuously growing interest as potential candidates for the replacement of traditional plastics.<sup>4,5</sup> To date, promising results have been obtained with bioplastics, in particular with the class of bio-based polyesters.<sup>6,9</sup> Their bio-based nature makes them particularly interesting for applications in food packaging field, since the multilayer structure of most of the packaging currently used creates severe recycling limits.<sup>10</sup> Nevertheless, to be suitable for food packaging employment, a polymeric device has to satisfy strict requirements, including proper mechanical response and outstanding barrier performance.<sup>11</sup> Nowadays, the so-called “smart packaging” has attracted a great interest too, as a result of lifestyle changes and consumer’s desire for convenient, safe and tasty food with prolonged shelf life and unaltered quality and freshness.<sup>12,13</sup> In these intelligent packaging systems, added materials interact with the internal environment of the package, monitoring the state of the food inside and reducing its corruption until consuming.<sup>14-16</sup> Another way to reduce environmental impact, is the use of flexible packaging instead of rigid one. A LCA study commissioned by Flexible Packaging Europe in 2021 showed that flexible packages have

67 a more than 60% lower impact than their rigid counterparts.<sup>17,18</sup> More in detail, using flexible  
68 alternatives means reducing package volumes and amount, saving space and energy during  
69 transportation and minimizing wastes. As a confirmation of this, another study, carried out by the  
70 Institute for Energy and Environmental Research in 2020, demonstrated that flexible packaging is  
71 more effective than rigid one in preserving resources and reducing carbon footprint: if all rigid  
72 packaging of non-beverage Fast Moving Consumer Goods in the European Union would be substitute  
73 by flexible one, the amount of primary packaging waste could be reduced by 21 million tonnes (i.e.  
74 70%) per year.<sup>18</sup>

75 In this framework, furan-based polyesters can be surely considered the materials of the future,<sup>19-24</sup>  
76 since they can be used to produce a mono-material packaging, combining bio-based origin<sup>25-31</sup> with  
77 excellent barrier properties and tunable mechanical performances, ranging from high stiffness to  
78 elastomeric behavior.<sup>32,33</sup> More important, they can also be recycled, once the first use has been  
79 accomplished.

80 When employed as food containers, plastics are often contaminated with organic matter, which  
81 prevents recycling, or at least makes it very expensive,. Moreover, it must be kept in mind that an  
82 efficient and sustainable plastic waste management became more complex and difficult due to  
83 COVID-19.<sup>34,35</sup> The pandemic emergency , has determined a huge increase of food packaging plastic  
84 waste due to online shopping and home delivery, accompanied by a change in mindset, according to  
85 which single use plastics provides “safety”. Plastic recycling increased at slower rate for fear that  
86 plastic wastes might be infected, and due to the lockdown too.<sup>36</sup>

87 Within this scenario, which was already complex and became even more difficult due to the  
88 pandemic, compostable packaging represents the best option, especially for single-use plastics.

89 Aromatic polymers, such as furan-based polyesters, are hardly attacked both by water and/or  
90 microorganisms.<sup>37-40</sup> The development of a strategy able to enhance their modest degradation rate is  
91 a really important challenge.<sup>41,42</sup>

As is well known, the strong point of plastics is the unique combination of light weight, durability, low cost, ease of synthesis and the possibility to *ad hoc* modify their functional properties in view of the particular application. Even though the use of additives, physical and chemical blending and production of composites are very effective tools to properly tune the material performances,<sup>24,43,44</sup> the starting point is definitely represented by a proper chemical design. Minor modifications in the chemical structure of a polymer, such as the overall composition, the atomic arrangement in the backbone, the length of the subunits in the repeating unit, the presence of side-groups and isomerism can lead to significant variations in physical properties.<sup>21,22,45-49</sup> Macromolecular mobility and the developed microstructure are strongly connected to the chemical structure of the polymer, thus affecting features like mechanical response, thermal stability, hydrophilicity, gas barrier performance and compostability.<sup>50</sup>

Considering also that 2,5-furandicarboxylic acid (FDCA) is one of 12 high value-added chemicals obtained from sugars<sup>31,51</sup> according to the United States Department of Energy (updated in 2020),<sup>52,53</sup> in the present work, a new 100% renewable furan-based polyester was synthesized by two-step melt polycondensation reaction, following the “Green chemistry” principles. For this purpose, FDCA has been coupled with diethylene glycol, recently proposed as bio-based monomer,<sup>54</sup> obtaining poly(diethylene 2,5-furanoate) (PDEF). It is worth noting that the starting monomers, FDCA and diethylene glycol, can be derived from second and third generation cellulosic feedstocks (non-food crops, waste materials and algae), thus avoiding the exploitation of food and animal feed as well as of land destined for food production.<sup>55</sup> As one can see from the PDEF chemical formula (**Scheme 1A**), an ether-oxygen atom is contained in its repeating unit. As previously evidenced for other polymeric systems,<sup>56-63</sup> the presence of -C-O-C- moiety in the polymer backbone has several effects, such as an increase in crystallinity degree decrease and wettability. These factors can potentially favour the water/polymer affinity and, consequently, the hydrolytic and bacterial attack of the macromolecule backbone. From the chemical structure point of view, PDEF can be considered as coming from the modification of the previously studied poly(butylene 2,5-furanoate) (PBF)<sup>33,64</sup> and

poly(pentamethylene 2,5-furanoate) (PPeF).<sup>32,33</sup> In particular, PDEF can be obtained through the insertion of an O atom (centrally located) in the glycol moiety of PBF, or by substituting the central methylene group of the aliphatic subunit of PPeF with the ether-oxygen (**Scheme 1A**). To the best of our knowledge, PDEF was previously synthesized by Katia Loos' group using a lipase as catalyst,<sup>65</sup> and by Haernvall et al. through direct esterification, and characterized from the molecular, thermal and enzymatic degradation point of view.<sup>66</sup> In addition to molecular and thermal characterization, the polyester reported in the present paper was also subjected to mechanical characterization and the surface hydrophilicity of the compression molded film was also evaluated. Lab-scale composting experiments were carried out at 58°C at 90% humidity. Barrier performances to oxygen and carbon dioxide were investigated at two different temperatures (23 and 38 °C). The effect of relative humidity at 23°C was also studied. All the results obtained for PDEF were compared with the previous ones got on PBF and PPeF with the aim to evaluate the effect of this chemical modification on the final solid-state properties. The present work is meant to enlarge the furan-based polymer knowledge and, more importantly, to lay the foundations for a deep study of structure-property relationship, which is fundamental for the design of new materials addressing the desired final properties.

## **2. Materials and methods**

### **2.1 Materials**

Dimethyl furan-2,5-dicarboxylate (DMF) (99%), diethylene glycol (DEG) (99%), titanium tetrabutoxide (TBT), and titanium isopropoxide (TIP) were reagent-grade products. All reagents were bought from Sigma-Aldrich, except DMF, which was supplied by Matrix Fine Chemicals.

### **2.2 Synthesis**

Poly(diethylene 2,5-furanoate) (PDEF) was synthesized through a green solvent-less two-stage polycondensation process. The reagents DMF (0.031 mol, 5.71 g) and DEG (0.062 mol, 6.58 g), in a molar ratio of 1:2, were charged in a 200 mL glass reactor, together with the catalysts TBT and TIP

(200 ppm of both). The system was continuously stirred (50 rpm) and the temperature adjusted by a silicone oil bath. A condenser cooled by liquid nitrogen was coupled to the reactor. In the first step, carried out at 180 °C and under nitrogen flow, the transesterification reactions took place and methanol was released off. After 90% of theoretical methanol was collected (i.e. 90 minutes), the pressure was progressively reduced to 0.05 mbar, while the temperature was raised up to 230 °C. In the second stage, lasting 3 hours, the reaction mass viscosity increased till a constant torque value. Afterwards, the polymer (6.5 g, 95% yield) was discharged from the reactor. A lightly coloured rubber-like solid was obtained. PBF and PPeF were previously synthesized by the authors through the same polycondensation procedure using the same catalysts.<sup>32,33</sup> Briefly, for PBF the glycolic molar excess was 300%, the first step was carried out at 180°C for 3 hours and the second one at 230°C for further 3 hours. In case of PPeF, a glycolic molar excess of 500% was adopted, the first step was carried out at 170°C for 3 hours while the second one at 220°C for further 2.5 hours. The as-synthesized polymer was solubilized in chloroform and then precipitated in cold methanol, in order to remove residual catalysts and low molecular weight by-products.

### 2.3 Molecular characterization

Polymer chemical structure was verified by <sup>1</sup>H-nuclear magnetic resonance spectroscopy (Varian Inova 400-MHz Instrument) at room temperature using deuterated chloroform (CDCl<sub>3</sub>) as solvent. The solution contains also 0.03 vol% tetramethylsilane (TMS) as an internal standard. The concentration of the polymeric solution was 0.5 wt %.

Polymer number molecular weight ( $M_n$ ) and polydispersity index ( $\mathcal{D}$ ) were determined by a 1100 HPLC system (Agilent Technologies) equipped with PLgel 5 mm MiniMIX-C column, at 30 °C. Chloroform was used as the eluent, 0.3 mL/min flow, and sample concentrations of about 2 mg/mL were adopted. Calibration curve was obtained using polystyrene standards in the range of 800–100000 g/mol.

### 2.4 Thermal characterization



Differential Scanning Calorimetry (Perkin Elmer DSC6), calibrated with indium and cyclohexane standards, was used to analyse the thermal transitions by heating from -70 °C to 190 °C at 20 °C/min (I scan, resolution: 0.1 seconds between points). The sample (5 mg) was then cooled to -70 °C at 100 °C/min, and after that another heating scan was performed (II scan, resolution: 0.1 seconds between points). The glass transition temperature ( $T_g$ ) and heat capacity ( $\Delta C_p$ ) were taken as the midpoint and the height, respectively, of the heat capacity step at the glass transition. Melting temperature ( $T_m$ ) and crystallization temperature ( $T_{cc}$ ) were determined as the peak maximum/minimum of the endothermic/exothermic phenomena in the I and II heating scan DSC curves, respectively. The corresponding heat of fusion ( $\Delta H_m$ ) and heat of crystallization ( $\Delta H_{cc}$ ) were obtained from the total area of the DSC endothermic and exothermic signals, during the I and the II heating scans, respectively. For the determination of  $\Delta H_m$  and  $\Delta H_{cc}$  we have used a straight baseline.

Thermogravimetric analysis (Perkin Elmer TGA7), was employed to evaluate the thermal stability by heating 5 mg of polymer from 50 to 800°C at 10°C/min under nitrogen atmosphere (gas flow: 40 ml/min). The maximum degradation rate temperature ( $T_{max}$ ) was calculated as the minimum of thermogram derivative .

## **2.5 Film preparation**

Polymer films (2.5 g, 11 x 11 cm<sup>2</sup>, 100 µm thickness) were obtained by compression molding the synthesized material with a laboratory press Carver C12. The polymer was heated to 100 °C, kept under 5 ton/m<sup>2</sup> pressure for 2 min, removed from the press and left cooled down to room temperature. Then, the films were stored at room temperature for 30 days before further characterization.

## **2.6 Water contact angle measurements**

Water contact angle (WCA) determination was carried out on the compression moulded films using a KSV CAM101 instrument (Helsinki, Finland) at room temperature. The side profiles of deionized water drops (4 µL) on the polymer surface were analyzed just after deposition. In case of PDEF, also

the drop shape evolution with time was considered. At least 10 tests have been performed on different film areas, from which the WCA average value  $\pm$  standard deviation was determined.

## **2.7 Mechanical characterization**

Tensile tests were performed on rectangular specimens (5 mm x 50 mm x 100  $\mu$ m) by means of an Instron 5966 testing machine with a transducer-coupled 1kN load cell (stretching rate: 10 mm/min). The measurements were carried out at room temperature (23  $^{\circ}$ C) and a relative humidity of 55%. Elastic modulus (E) was calculated from the initial slope of the stress-strain curve. Stress at yielding ( $\sigma_y$ ) and stress ( $\sigma_b$ ) and elongation ( $\epsilon_b$ ) at break were also determined. These results are reported as the average value  $\pm$  standard deviation, obtained testing six different specimens.

## **2.8 Barrier properties**

Barrier capability to oxygen and carbon dioxide was evaluated by a manometric method using a Permeance Testing Device, type GDP-C (Brugger Feinmechanik GmbH), according to ASTM 1434-82, DIN 53 536 and ISO/DIS 15 105-1 protocol. The measurements were performed on a film surface of 78.5 cm<sup>2</sup>, under a gas stream of 100 cm<sup>3</sup>/min, at 23 and 38  $^{\circ}$ C, and 0 and 85 % relative humidity. The results have been expressed as gas transmission rate (GTR, in cm<sup>3</sup> cm m<sup>2</sup> d<sup>-1</sup> atm<sup>-1</sup>), which defines the permeability to gas of the film. The measurements were made in triplicate and the result was expressed as average value  $\pm$  standard deviation.

## **2.9 Composting tests**

Composting studies have been carried out at 58  $^{\circ}$ C in mature compost kindly supplied by HerAmbiente S.p.A. Films of about 20x20 mm<sup>2</sup> (50 mg) were placed in a 100 mL bottle containing wet compost. Specimens were withdrawn from compost in triplicate at different time intervals, washed and dried over P<sub>2</sub>O<sub>5</sub>.

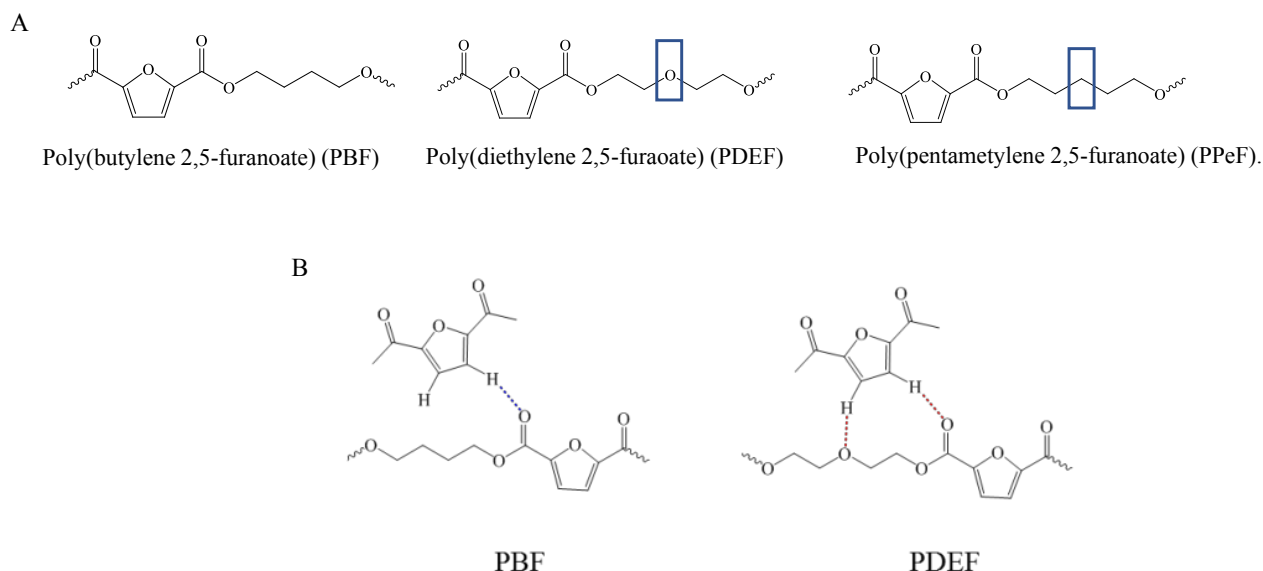
## **2.10 SEM investigation**

215 Surface characterization was carried out by scanning electron microscopy (SEM). SEM images were  
216 acquired on a desktop Phenom microscope on metal sputtered film samples glued on aluminum  
217 holders with carbon tape.

### 218 3. Results and discussion

#### 219 3.1 Molecular characterization

220 In **Scheme 1A**, the chemical structure of poly(diethylene 2,5-furanoate) (PDEF) is reported, together  
221 with the formulas of the two homopolymers poly(butylene 2,5-furanoate) (PBF) and  
222 poly(pentamethylene 2,5-furanoate) (PPeF) to which PDEF has been compared throughout the  
223 present study. All the polyesters present a furan ring in the acid subunit, the difference being in the  
224 glycolic moiety. In case of PBF, four methylene groups are present. PDEF has the same number of -  
225 CH<sub>2</sub>- groups, plus an ether-oxygen atom in between, this latter replaced by a methylene group in case  
226 of PPeF. PDEF could be considered as derived, on one side from PBF by the insertion of a central O  
227 atom in the glycol moiety and, on the other, from PPeF by the substitution of the central -CH<sub>2</sub>- group  
228 with a -O- one.



229 **Scheme 1. A)** Molecular structures of poly(diethylene 2,5-furanoate) (PDEF), poly(butylene 2,5-  
230 furanoate) (PBF) and poly(pentamethylene 2,5-furanoate) (PPeF); **B)** Inter-chain hydrogen bonds in  
231 PBF and PDEF matrices. For PPeF, a PBF-like behaviour was also supposed.  
232

233

234 In **Fig. S1** the PDEF <sup>1</sup>H-NMR spectrum, together with the spectra of PBF and PPeF, is reported. As  
235 one can see, the expected structure for PDEF was confirmed. In details, the -CH<sub>2</sub>- groups of the  
236 diethylene glycolic unit gave rise to two triplets at 3.82 (f) and 4.49 ppm (e), while the two d protons  
237 proper of the furan ring produced a singlet (a) located at 7.20 ppm. PBF showed the same signal at  
238 7.34 ppm (a), then the peaks of the b and c methylene groups of the butylene subunit could be  
239 observed at 4.51 and 1.99 ppm, respectively. PPeF, beside the furan ring signal (g) at 7.20 ppm,  
240 presented three different peaks due to the methylene hydrogen atoms at 4.35 (h), 1.84 (i) and 1.57  
241 ppm (j). The high molecular weight, obtained by means of GPC and reported in **Table 1**, confirmed  
242 the good control of the PDEF synthetic route, analogously to PBF and PPeF homopolymers.<sup>33</sup> The  
243 polydispersity index (Đ) resulted close to 2, as expected for a polycondensation process.  
244 The use of traditional Titanium-based catalysts has made possible to obtain a polymer with a  
245 significantly higher molecular weight than that previously obtained by others using a lipase as  
246 catalyst.<sup>65</sup>

### 247 **3.2 Thermal characterization**

248 TGA analysis has been carried out to follow PDEF weight loss during heating scan under inert  
249 atmosphere (nitrogen). The corresponding thermogravimetric curve is reported in **Fig. 1A**, together  
250 with those previously obtained for PBF and PPeF, while the corresponding T<sub>max</sub> values are listed in  
251 **Table 1**. The derivative curves of thermograms are reported in **Fig. S2**. It is worth noticing the high  
252 thermal stability of all the furan-based polyesters here evaluated.

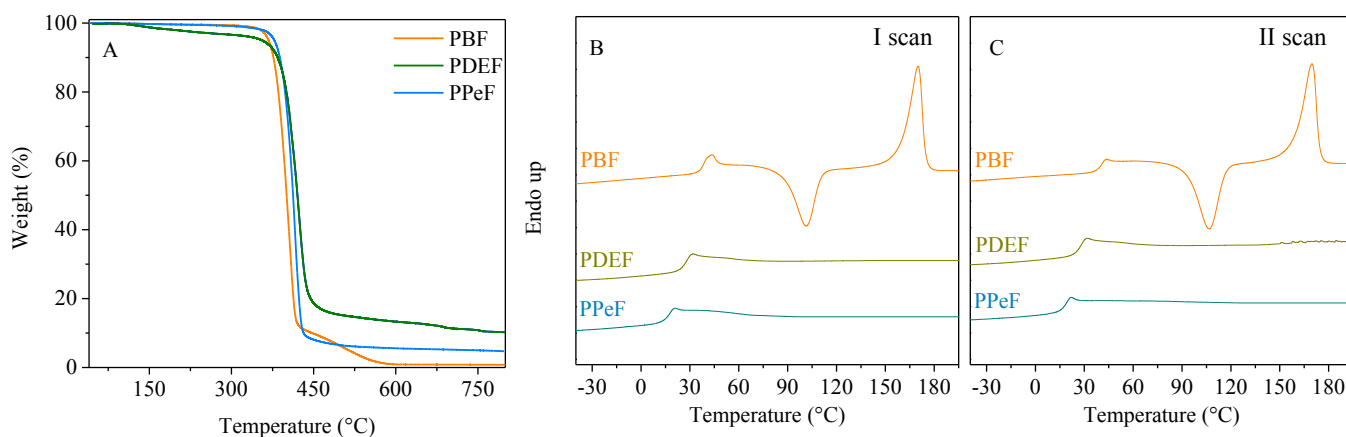


**Fig. 1. A)** Thermogravimetric analysis curves of PBF, PDEF and PPeF samples obtained by heating at 10°C/min under nitrogen atmosphere; **B)** DSC traces of first heating scan of the compression moulded films and **C)** second heating scan after melt quenching (20 °C/min) of PBF, PDEF, PPeF.

In agreement with previous studies,<sup>67-69</sup> PBF degraded at lower temperature (and comparable to the one evidenced by Kainulainen et al.<sup>64</sup>) compared with the other two samples, reaching the maximum degradation rate at 407°C, while PDEF had the highest stability despite an initial weight loss of 4% occurring at approximately 100°C. The presence of -O- ether linkages along the macromolecular backbone, in fact, increased the tendency of the material to absorb polar molecules as water. The evaporation of the adsorbed H<sub>2</sub>O molecules could be likely responsible for this initial weight loss step in PDEF. The highest  $T_{max}$  value obtained for PDEF could be due to the higher energy of the C-O bond, present in the diethylene glycol moieties, less prone to random scission compared with C-C bond (358 kJ/mol vs. 346 kJ/mol, respectively<sup>70</sup>), proper of PBF and PPeF. Another important aspect was related to the formation of inter-chain hydrogen bonds, as shown in **Scheme 1B**. The establishment of inter-chain hydrogen bonds for furan-based polyesters, in addition to  $\pi$ - $\pi$  interaction between the aromatic rings, has been evidenced by dielectric experiments, rheological analysis<sup>71</sup> and lastly proposed through simulation studies.<sup>72</sup> Considering the chemical structure, one can hypothesize that the presence of an ether-oxygen atom in the PDEF unit could increase the hydrogen bond density, thus improving the thermal resistance of the material, since the energy provided to polymer chains,

during heating, is first and preferentially used to break these physical links before breaking covalent bonds. On the contrary, the lowest thermal stability of PBF among all the samples under study could be ascribed to the lowest number of hydrogen bonds. The glassy state of PBF at room temperature could limit the establishment of such inter-chain interactions, since at 25 °C, the PBF polymer chains have lower molecular mobility than those of the rubbery PPeF sample.

Calorimetric analysis was performed in order to define the thermal transitions proper of the three samples subjected to compression molding. The DSC traces and the relative data are reported in **Fig. 1** and in **Table 1**, respectively. The cooling scans between I and II heating scans reported in **Fig. S3**. PBF film presented a melting peak centered at 164°C and preceded by a cold crystallization endotherm located at 87°C; since  $\Delta H_m > \Delta H_{cc}$ , PBF film could be considered as semicrystalline. PDEF and PPeF did not present any melting peaks, showing no capability of organizing their macromolecules in crystalline structure through the compression molding process, in agreement with previous studies.<sup>32,73</sup> Just a glass transition step, respectively at 24 °C and 13 °C, was observed; in both cases, the values recorded were lower than the PBF one. Looking at the chemical formulas of **Scheme 1A**, one can see that PDEF and PPeF are characterized by longer glycolic subunits (PDEF: 4 -CH<sub>2</sub>- and 1 -O-; PPeF: 5 -CH<sub>2</sub>- moieties) compared with PBF (4 -CH<sub>2</sub>- moieties). Even if the nature of the atom changes, longer glycols favor macromolecular mobility, moving  $T_g$  towards lower temperature.<sup>74</sup>  $T_{g,PDEF}$  can be compared with  $T_{g,PPeF}$ , due to their common fully amorphous nature. As one can see,  $T_{g,PDEF} > T_{g,PPeF}$ , the difference due to the high electronegativity of heteroatoms in the glycolic unit of PDEF, favouring inter chain interactions (reduced chain mobility).

Despite the comparable aliphatic segment length, the highly electronegative oxygen in the glycolic portion of PDEF promoted inter-chain interactions (hydrogen bonds as well as Van der Waals interactions). In this way, the segmental relaxation was hampered, and thus glass transition temperature increased.

298

299 **Table 1.** Molecular, thermal and mechanical characterization data of PDEF, PBF and PPeF films.

300 WCA (°) and GTR values to oxygen and carbon dioxide at 23°C, RH 0% are also collected.

			PBF	PDEF	PPeF
GPC		M <sub>n</sub> [g/mol]	27300 ±100	21400 ±100	29600 ±100
		Đ	2.3 ±0.1	2.3 ±0.1	2.4 ±0.1
TGA		T <sub>MAX</sub> [°C]	407 ±1	418 ±1	414 ±1
DSC	I SCAN	T <sub>g</sub> [°C]	39 ±1	24 ±1	13 ±1
		ΔC <sub>p</sub> [J/g·°C]	0.24±0.01	0.45±0.01	0.39±0.01
		T <sub>cc</sub> [°C]	102 ±1	/	/
		ΔH <sub>cc</sub> [J/g]	26 ±1	/	/
		T <sub>m</sub> [°C]	170 ±1	/	/
		ΔH <sub>m</sub> [J/g]	35 ±1	/	/
	II SCAN	T <sub>g</sub> [°C]	39 ±1	24 ±1	13 ±1
		ΔC <sub>p</sub> [J/g·°C]	0.28±0.01	0.47±0.01	0.43±0.01
		T <sub>cc</sub> [°C]	107 ±1	/	/
		ΔH <sub>cc</sub> [J/g]	30 ±1	/	/
		T <sub>m</sub> [°C]	170 ±1	/	/
		ΔH <sub>m</sub> [J/g]	35 ±1	/	/
Tensile test		σ <sub>y</sub> [MPa]	11 ± 2	7 ± 1	/
		σ <sub>b</sub> [MPa]	21 ± 3	4 ± 0.2	6 ± 1
		ε <sub>b</sub> [%]	157 ± 10	502 ± 100	1050 ± 200
		E [MPa]	1290 ± 140	673 ± 76	9 ± 1
WCA		Θ [°]	90 ± 2	74 ± 1	93 ± 3
Barrier properties		O <sub>2</sub> -TR [cm <sup>3</sup> cm / m <sup>2</sup> d atm]	0.10 ± 0.006	0.0022 ± 0.0002	0.0016 ± 0.0001
		CO <sub>2</sub> -TR [cm <sup>3</sup> cm / m <sup>2</sup> d atm]	0.19 ± 0.01	0.0018 ± 0.0001	0.0014 ± 0.0001

301

302

303 The three molten samples were subjected to fast cooling and analysed during a second heating  
304 measurement. As expected, PDEF and PPeF resulted again completely amorphous. As concerns PBF,  
305 a major polymer fraction could be quenched in the amorphous phase thanks to the high cooling rate,  
306 even though no completely amorphous sample could be obtained. As evidenced by II scan DSC trace,  
307 once  $T_g$  was exceeded, PBF macromolecules were able to fold in an ordered structure ( $T_{cc} = 107\text{ }^{\circ}\text{C}$ ;  
308  $\Delta H_{cc} = 30\text{ J/g}$ ) which melts at higher temperature ( $T_m = 170\text{ }^{\circ}\text{C}$ ;  $\Delta H_m = 35\text{ J/g}$ ). Despite the high cooling  
309 rate,  $\Delta H_m$  still keeps slightly higher than  $\Delta H_{cc}$ .

### 310 **3.3 Mechanical characterization**

311 Stress-strain measurements were conducted on PDEF films. The obtained curve is reported in **Fig. 2**,  
312 while the related data are collected in **Table 1**, together with the results previously got for PBF and  
313 PPeF samples. In details, PBF film showed high elastic modulus and stress at break, and quite low  
314 deformation at break in line with its semicrystalline nature, together with a  $T_g$  above room  
315 temperature. Differently, thanks to its amorphous nature and a  $T_g$  below room temperature, PPeF was  
316 characterized by an elastic modulus reduced by two orders of magnitude, together with an outstanding  
317 elongation at break (more than 1000 %). Moreover, as previously reported,<sup>32</sup> PPeF was able to recover  
318 its initial shape thanks to a supramolecular 1-D, 2-D structure springing from inter-chain hydrogen  
319 bonds established between macromolecular chains. PDEF had a mechanical behavior intermediate  
320 between the one typical of a semicrystalline material, as PBF, and that of a rubbery fully amorphous  
321 polymer, as PPeF. Like PBF, PDEF undergoes yielding,<sup>75,76</sup> a phenomenon which was not observed  
322 in PPeF. The lack of crystallites in PDEF produced a reduction of  $E$  and  $\sigma_y$  compared to PBF. This  
323 decrement was contained by the interactions among different chains, thanks to the oxygen atom of  
324 the glycolic subunit, which helped keeping the elastic modulus and the strain before yielding quite  
325 high. At the same time, the higher chain mobility of PDEF with respect to PBF (lower  $T_g$ ), coming  
326 from the introduction of O atom, allowed reaching a 500%  $\epsilon_b$ .



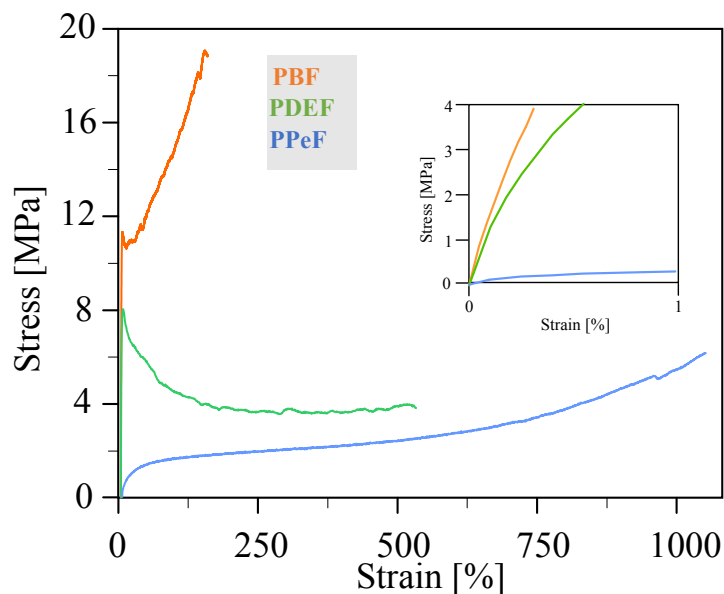


**Fig. 2.** Stress-strain curves of PBF, PDEF and PPeF films. In the inset the region corresponding to low values of stress and strain is reported.

### 3.4 Water contact angle

In order to evaluate the surface hydrophilicity of PDEF film, the interaction between film and water was investigated through water contact angle measurements. Particular attention was devoted to the effect of the introduction of an oxygen atom in the polymer backbone. Again, the outcomes obtained for PDEF film have been compared with the PBF and PPeF ones.

As it is clearly visible from **Fig. 3A** and from the data in **Table 1**, PDEF resulted the most hydrophilic film, being the  $WCA_{PDEF}$  lower than both  $WCA_{PBF}$  and  $WCA_{PPeF}$ . These results suggest that the introduction of ether-oxygen in the PBF repeating unit increases the polarity of the material, as already suggested by previous studies.<sup>77</sup>

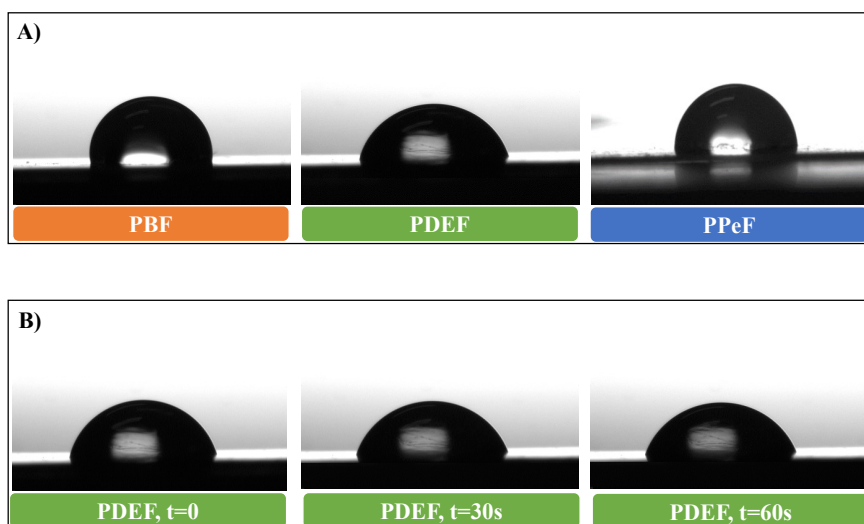


**Fig. 3. A)** Images of water drops deposited on PBF, PDEF and PPeF films; **B)** water drop on PDEF after 0, 30 and 60 s from deposition.

The high affinity with water was in line with the TGA results obtained for PDEF. The initial weight loss observed during the thermogravimetric analysis can be ascribed to the release of the humidity absorbed from the environment. By replacing the oxygen atom of the PDEF glycolic subunit with a non-polar  $-\text{CH}_2-$  group, obtaining the PPeF chemical structure, the hydrophobic character rose again. WCA value of PPeF is similar to that of PBF, despite the greater length of the aliphatic portion (4  $-\text{CH}_2-$  for PBF vs. 5  $-\text{CH}_2-$  for PPeF).

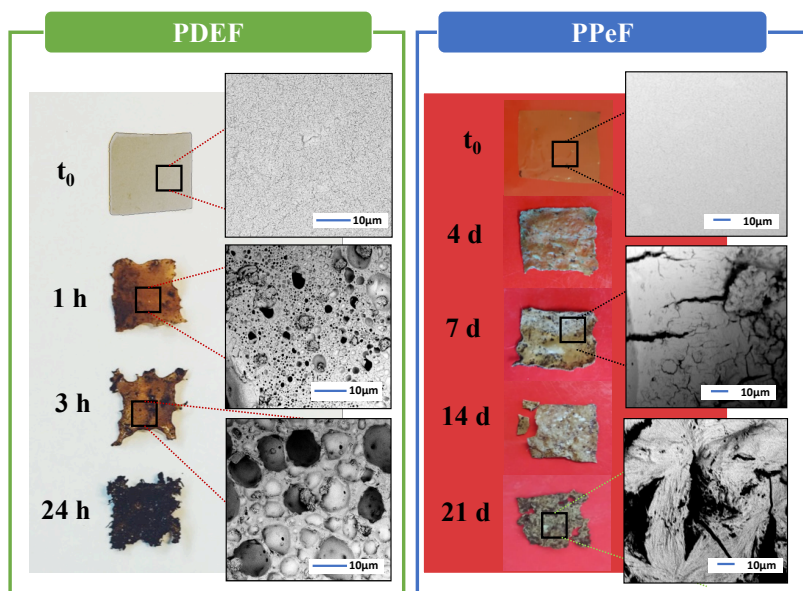
In **Fig. 3B**, the profile change of the drop deposited on PDEF film as a function of time was reported. A clear difference in contact angle could be observed just after 30 s from the release of the water drop. A completely different behaviour was observed for PPeF and PBF, for both of which no evolution of the drop shape with time was detected. The drop shape evolution on PDEF surface is further evidence of its improved hydrophilicity with respect to PBF and PPeF.

### 3.5 Composting test

In order to evaluate the potential end-of-life destination of PDEF-based products, composting tests were conducted. For each sample, square shaped films were incubated in adequately prepared compost and maintained under controlled atmosphere (58°C, 90% relative humidity). Then, several

358 withdrawals were operated at different times (**Fig. 4**). The composting measurements were also  
 359 carried out on PBF and PPeF samples. As regards PBF, after 62 days in compost, no changes on the  
 360 film surface nor in the gravimetric weight were observed.

361



362

363 **Fig. 4.** PDEF and PPeF film images collected at different composting times: macroscopic view (left)  
 364 and SEM images (right).

365

366 A deeply different behaviour was observed for PDEF, which underwent degradation as soon as  
 367 incubated (**Fig. 4**). Just after 1 hour, the film macroscopically changed in colour and dimension, holes  
 368 and cracks were clearly observed with SEM. In particular, the cavities increased in size with the  
 369 incubation time, and after just 3 hours, the surface was almost completely covered of holes. After 24  
 370 hours of incubation, the film was wholly incorporated in compost. The high tendency to degrade  
 371 comes from the high hydrophilicity of PDEF given by the oxygen atoms inserted in the glycolic  
 372 subunit, and from the rubbery state of the polymer under the experimental conditions. Both these  
 373 features favour the diffusion of water molecules and microorganisms' attack. It is worth noting that  
 374 PDEF film did not undergo solubilization, as confirmed by additional experiments carried out in neat  
 375 water. In this case, no changes in PDEF film both at micro- and macroscopic level were observed,

even after months. As concerns PPeF, its degradation proceeded very fast, but at lower extent compared with PDEF. Also in this case  $T_{\text{incubation}} > T_{g,\text{PPeF}}$ , but degradation was slowed down likely because of the lower hydrophilicity. Anyway, after 4 days, macroscopical changing on the film surface could be seen and, after 7 days, cracks and holes could be observed microscopically via SEM analysis. In 21 days, the film was deeply compromised by degradation process both at micro- and macroscopic level (**Fig. 4**). Given the compost contamination of the incubated PDEF and PPeF films, it was not possible to perform weight loss measurements.

The huge slowing down of composting rate for PBF films has to be ascribed to its semicrystalline nature and lower macromolecular mobility ( $T_{g,\text{PBF}} > T_{g,\text{PDEF}}, T_{g,\text{PPeF}}$ ) more than to its quite high hydrophobicity, being this last comparable to PPeF one ( $\text{WCA}_{\text{PBF}} \approx \text{WCA}_{\text{PPeF}}$ ).

### 3.6 Barrier properties

Barrier properties are influenced by several factors that can have different impact on the final performance. As a general trend, all factors that increase free volume among chains worsen barrier properties. A pertinent example is the macromolecule flexibility, which is related to the glass transition temperature. In particular, the lower the  $T_g$  the higher the number of unoccupied spaces, which cause the increase of gas transmission rate (GTR). Differently, the presence of ordered phases hampers the passage of gases through the film. In addition to the three-dimensional crystals, in the systems containing aromatic or aliphatic rings connected by flexible moieties, 1D- and 2D-ordered phases can develop, arising from Van der Waals forces,  $\pi$ - $\pi$  stacking and polar interactions.<sup>78-82</sup> Barrier properties also depend on the possibility of ring flipping,<sup>83</sup> and of macromolecular arrangements, which may affect the overall dipolar moment without changing the chemistry.<sup>84</sup> In addition to them, in the case of furan-based polymers, the establishment of hydrogen bonds can be also considered.<sup>32,33,71,72</sup> PDEF gas barrier properties were analysed and compared with those of PBF and PPeF.

The permeability performances to two different pure gases,  $\text{O}_2$  and  $\text{CO}_2$ , were evaluated on the compression moulded films. In **Fig. 5A** the results, expressed as gas transmission rate (GTR), were

402 reported. The experiments were conducted sequentially, as follows: i) temperature (T) 23°C, relative  
403 humidity (RH) 0%; ii) T 23°C, RH 85%; iii) T 23°C, RH 0%. From the first test conducted at 23°C  
404 in dry atmosphere, it was clear that PBF presented the highest values of GTR among the series, despite  
405 its higher glass transition temperature and semicrystalline nature. Differently, PDEF and PPeF, even  
406 though amorphous and with  $T_g$  values around the temperature of measuring, resulted very outstanding  
407 and with comparable performance. An explanation could be found, as mentioned before, in the  
408 presence of a particular macromolecular arrangement that blocked the passage of gases through the  
409 materials.<sup>85</sup> In the case of PPeF, as previously reported,<sup>32,33</sup> 1-D, 2D-ordered domains developed  
410 during compression moulding with consequent improvement of gas barrier performance. This  
411 peculiar microstructure originated from inter-chain hydrogen bonds, these last also present, and to  
412 greater extent, in PDEF. The presence of ether-oxygen atom in PDEF repeating unit enhanced the  
413 number of hydrogen bonds favouring the inter-molecular forces. These last lead to a compact array,  
414 that hampered the gas molecules passage. At the same time, the insertion of an oxygen atom into the  
415 glycol subunit decreases the symmetry of the aliphatic segment, reducing the macromolecular sorting.  
416 In other words, the density of the inter-chain hydrogen bond increases due to the presence of ether O  
417 atoms, but their random distribution determines a not enough long chain arrangement, not detectable  
418 through diffractometric measurements. Nevertheless, unexpectedly, the barrier performances of the  
419 PDEF were not superior to those of PPeF. The result could be explained considering that the  
420 formation of the compact array is somewhat contrasted by the lower mobility of the PDEF  
421 macromolecular chains compared to those of the PPeF ( $T_{g,PDEF} > T_{g,PPeF}$ ).  
422 Afterwards, the three films were subjected to permeability tests at 85% RH, keeping the temperature  
423 constant at 23°C. In case of PBF, an improvement of barrier performance was observed, while for  
424 PDEF, permeability values remained almost constant. The result was quite surprising considering the  
425 usually observed plasticizing effect of water, which, enhancing the chain mobility, determined an  
426 increment of the free volume. On the other side, the same plasticizing effect detected for PPeF, caused  
427 a slight increase of GTR values under humid conditions. To explain the behaviour of PDEF and PBF

428 films, it was supposed that water enhanced the inter-chain interactions occupying the empty sites at  
429 the oxygen atoms of the furan ring and, in case of PDEF, also at the oxygen of the glycolic subunit.  
430 Hence, a more compact and dense new structure was formed, responsible for the decreasing of the  
431 GTR values.<sup>85</sup> In the case of PPeF, also containing furan O atoms in the furan ring, the longer glycolic  
432 part compared to PBF decreased the density of furan ring per unit length. Therefore, the plasticizing  
433 effect of water prevailed on the formation of a more compact microstructure arising from the  
434 hydrogen bonds establishment. In PDEF, characterized by repeating unit length comparable to PPeF,  
435 the presence of the oxygen atom instead of the central methylene group explained the different  
436 behaviour in wet environment.

437 In the third experiment, the films were firstly subjected to vacuum in order to remove the moisture  
438 residues and then, a new test was performed at 23°C and 0% RH. PBF and PDEF maintained the  
439 same good performances reached under humid conditions. It is plausible that the vacuum applied was  
440 not affecting the hydrogen bonds formed among water and furan/ether oxygen. For PPeF, it could be  
441 hypothesized that the free molecules of water trapped inside the material and acting as plasticizer,  
442 were removed by vacuum. Conversely, those forming hydrogen bonds with the furan ring remained  
443 inside the material, making GTR-O<sub>2</sub> value decrease and GTR-CO<sub>2</sub> one almost unvaried.

444 Another aspect to consider was the different perm-selectivity ratio, defined as  $GTR_{CO_2}/GTR_{O_2}$ , which  
445 is an indication of the different barrier performance towards the two gases. It should be remembered  
446 that oxygen is a small and no-polar molecule characterized by a transmission rate lower than that of  
447 the larger carbon dioxide, which contains polar C-O covalent bonds.<sup>50</sup> Consequently, the perm-  
448 selectivity ratio is usually higher than 1. Usually, in polyesters  $GTR_{CO_2} > GTR_{O_2}$ , meaning carbon  
449 dioxide passed through the films easier than O<sub>2</sub>. In the furan-based polyesters, a peculiar behaviour  
450 with particularly low GTR values for CO<sub>2</sub> had been documented.<sup>32,86-88</sup> This evidence was ascribed  
451 to the presence of permanent dipoles in CO<sub>2</sub> interacting with the polar groups of polymeric chains

(furan ring), thus increasing CO<sub>2</sub> solubility and simultaneously decreasing its diffusivity. The consequent result is a GTR<sub>CO<sub>2</sub></sub>/GTR<sub>O<sub>2</sub></sub> ratio close to 1 for furan-containing polyesters.

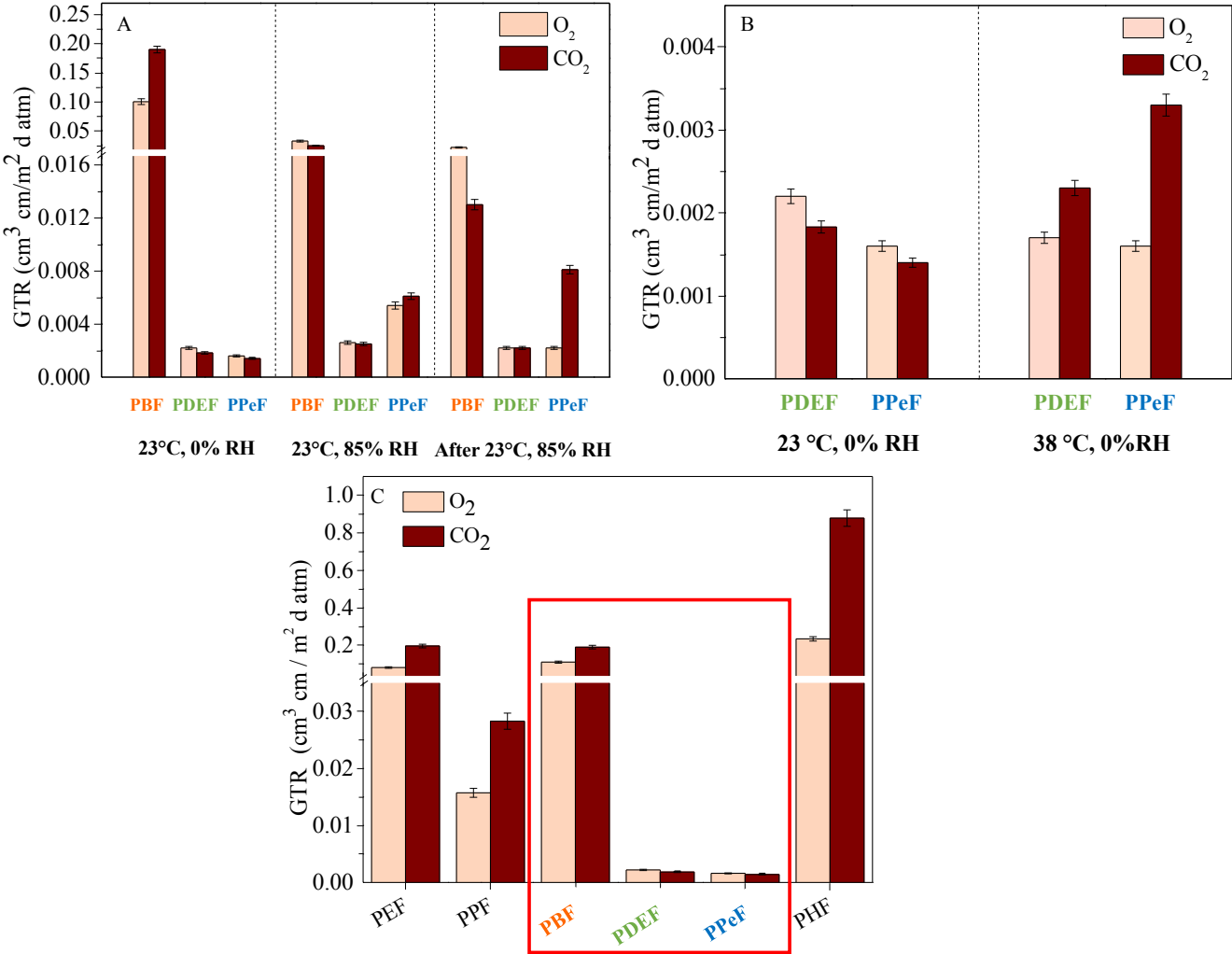


**Fig. 5. A)** GTR-O<sub>2</sub> and -CO<sub>2</sub> of PBF, PDEF and PPeF, for three subsequent experiments conducted at 23°C in different conditions of humidity; **B)** GTR-O<sub>2</sub> and -CO<sub>2</sub> of PDEF and PPeF at 23 and 38 °C; **C)** GTR-O<sub>2</sub> and -CO<sub>2</sub> of different furan-based polyesters (PEF<sup>34</sup>, PPF<sup>10</sup>, PHF<sup>10</sup>).

Considering the three-step experiment reported in **Fig. 5A**, a different effect of humidity conditions on perm-selectivity ratio could be found for PBF, PDEF and PPeF films.

463 As concerns PBF, in the first test conducted, the driving force was the dimension of the molecules.  
464 Operating at 85% RH, new polar interactions between water molecules and polymer chains formed,  
465 favouring CO<sub>2</sub> solubility. The effect kept constant even returning to dry environment.  
466 In case of PDEF, its higher polarity due to the O atom insertion in the PBF backbone, helped to  
467 maintain the  $GTR_{CO_2}/GTR_{O_2}$  ratio always close to 1. As regards PPeF, the trend observed was  
468 different: humidity determined an increment of perm-selectivity ratio, which further increased after  
469 removing free water molecules by vacuum. This trend could be explained considering that H<sub>2</sub>O first  
470 acted as plasticizer, enhancing polymer chain mobility, and then left vacancies after vacuum was  
471 applied. Both these effects increased the free volume, favouring mainly the passage of the fastest CO<sub>2</sub>  
472 molecules. These last, in turn, were less soluble in PPeF than in PBF and especially in PDEF films.  
473 PDEF and PPeF were also tested at 38°C to simulate hot weather conditions. As one can see from  
474 **Fig. 5B**, despite at this temperature macromolecular chains of both polymers were in a complete  
475 mobile state, barrier properties did not suffer a general worsening. This experiment supports, one  
476 more time, the hypothesis of supramolecular arrays originated from hydrogen bonds among the  
477 chains. As evident, these compact structures were not affected by the increasing of temperature, since  
478 the polymers maintain their performances. Differently, the increase of temperature in case of common  
479 polyesters leads to higher free volume among the macromolecules, favouring gas permeation.  
480 Anyway, an increase of CO<sub>2</sub> gas transmission rate was detected by increasing temperature. As already  
481 mentioned, the gas passage depended on both solubility and diffusivity. This latter generally rises  
482 with temperature, the effect being more intense for the gas molecules characterized by the most  
483 chaotic motions, such as CO<sub>2</sub> molecules. In both cases, the performances to O<sub>2</sub> at 23°C and 38°C  
484 were constant, while  $GTR_{CO_2}$  values increased.  
485 In **Fig. 5C**, a comparison of PDEF with PBF, PPeF and other furan-based polyesters was reported.  
486 As one can see, PDEF and PPeF had GTR values much lower than the other materials.



487 In addition, an odd/even effect could be observed: the materials with odd number of -CH<sub>2</sub>- groups  
488 resulted more performant compared to the even numbered -CH<sub>2</sub>- containing ones. Surprisingly, PDEF  
489 and PPeF presented GTR values lower than those of PPF, despite their lower T<sub>g</sub> (T<sub>g,PPeF</sub> = 13°C;  
490 T<sub>g,PDEF</sub> = 24°C; T<sub>g,PPF</sub> = 52°C). As previously reported, the deviating behaviour of PPeF and PDEF  
491 could be attributed to the supramolecular compact phase coming from the hydrogen bond formation,  
492 this last being favoured in rubbery amorphous furan-polyesters as PDEF and PPeF.  
493 As regards the materials containing an even number of -CH<sub>2</sub>- groups, PEF, PBF and PHF, a  
494 progressive worsening of gas barrier performances can be observed, ascribable to different reasons  
495 as previously reported:<sup>33,89</sup> (i) increasing amount of the so called disclinations; (ii) increasing fraction  
496 of 3D-ordered phase at the expense of the more performant 2D-one; (iii) increasing of free volume  
497 fraction (T<sub>g,PEF</sub> > T<sub>g,PBF</sub> > T<sub>g,PHF</sub>).

#### 498 **4. Conclusions**

499 The use of traditional synthetic Ti-based catalysts together with an optimized solvent-free two-stage  
500 polycondensation process permitted to obtain a 100% bio-based high molecular weight  
501 poly(diethylene 2,5-furanoate) (PDEF). The polymer could be processed in form of thin freestanding  
502 films by compression moulding, although completely amorphous and with a T<sub>g</sub> around room  
503 temperature. A similar behaviour was previously observed for poly(pentamethylene 2,5-furanoate)  
504 (PPeF), with respect to which the polymer object of this study has some important similarities in  
505 terms of properties. In particular, both polyesters are characterized by very high thermal stability  
506 (PDEF's one even slightly higher than that of PPeF), exceptional gas barrier properties both at room  
507 temperature and at 38°C, preserved in the presence of humidity. Lastly, they are both compostable,  
508 although PDEF degrades much faster than PPeF, mainly due to its greater hydrophilicity. In terms of  
509 mechanical response, a fundamental property for a possible application in food packaging, PDEF  
510 showed an intermediate behaviour between poly(butylene 2,5-furanoate) (PBF) and PPeF. In fact,  
511 PDEF film exhibited the flexibility typical of PPeF, even though not an elastomeric behaviour (PDEF

512 stress-strain curve shows yielding), but a much higher elastic modulus and stress at break as PBF,  
513 which confer to the material toughness and ductility. Therefore, with PDEF both the mechanical  
514 limits of PBF (brittleness) and of PPeF (too high softness) are overcome, without compromising the  
515 outstanding thermal stability, gas barrier properties and compostability of PPeF. The goal was  
516 achieved through a small chemical modification of polymer chemical structure, i.e. the insertion of  
517 an ether oxygen atom into the glycol subunit, centrally positioned. As known from basic chemistry,  
518 oxygen is characterized by high electronegativity and small dimensions, and these characteristics  
519 have had a significant impact on the final properties of the polymer. Specifically:

- 520 - The lower dimension of oxygen with respect to carbon atom affected the chain constitutional  
521 regularity with consequent suppression of the polymer crystallization capacity (PDEF is  
522 amorphous, whereas PBF is semicrystalline). Moreover, C-O bond is shorter than C-C one,  
523 implying for ethereal bond a higher energy (PDEF is more thermally stable than PBF); the  
524 insertion of an oxygen atom in glycol subunit also makes its polymer chain more flexible than  
525 that of PBF, the aliphatic part being longer;
- 526 - The high oxygen electronegativity strengthens inter-chain interactions (hydrogen bonds  
527 involving furan ring and Van der Waals interactions) responsible of the outstanding gas  
528 barrier (similar to those of PPeF) and mechanical properties (better than those of both PBF  
529 and PPeF) and increases polymer hydrophilicity, the parameter determining the very fast  
530 compostability of this polyester.

531 In conclusion, PDEF represents a very promising candidate to obtain an easily recyclable mono-  
532 material package and also for producing single-use plastic packaging compostable in just one day.

533

## 534 **Author contributions**

535 S.Q. M.S. synthesized and characterized the polymer. V.S. performed gas barrier measurements.  
536 S.Q., G.G., M.S. and N.L. analyzed the overall experimental data. M.S. and N.L. wrote manuscript.  
537 G.G., M.S. and N. L. corrected and reviewed the manuscript. N.L. supervised and financed the work.

## 538 **Conflicts of interest**

539 The authors declare no conflict of interests.

## 540 **Acknowledgments**

541 S.Q, G.G., M.S., N.L., and V.S. acknowledge the Italian Ministry of University and Research. This  
542 publication is based upon work from COST Action FUR4Sustain, CA18220, supported by COST  
543 (European Cooperation in Science and Technology).

544 The authors thank Dr. Massimo Gazzano for his cooperation in the acquisition of SEM micrographs.

## 545 **Supplementary data**

546 These files can be found in the supplementary data:

547 Fig. S1. <sup>1</sup>H-NMR spectra of PBF, PDEF and PPeF (from the top to the bottom) with the relative peak  
548 assignment.

549

## 550 **References**

- 551 1. Plastics - The facts 2020. *PlasticsEurope*, 2020,  
552 <https://www.plasticseurope.org/en/resources/publications/4312-plastics-facts-2020> (accessed  
553 [July 2021](#)).
- 554 2. <https://www.statista.com/statistics/664906/plastics-production-volume-forecast-worldwide/>  
555 [STATISTA 2021](#) (accessed [September 2021](#)).
- 556 3. Plastic Market Size, Share & Trends Analysis Report by Product (PE, PP, PU, PVC, PET,  
557 Polystyrene, ABS, PBT, PPO, Epoxy Polymers, LCP, PC, Polyamide), by Application, by

- End-use, by Region, and Segment Forecasts, 2021 – 2028, Grand view Research 2021 (accessed: September 2021).
4. RameshKumar, S.; Shaiju, P.; O'Connor, K. E.; P, R. B. Bio-Based and Biodegradable Polymers - State-of-the-Art, Challenges and Emerging Trends. *Curr. Opin. Green Sustain. Chem.* **2020**, *21*, 75–81.
  5. Mülhaupt, R. Green Polymer Chemistry and Bio-based Plastics: Dreams and Reality. *Macromol. Chem. Phys.* **2013**, *214*, 159–174.
  6. Rabnawaz, M.; Wyman, I.; Auras, R.; Cheng, S. A roadmap towards green packaging: the current status and future outlook for polyesters in the packaging industry. *Green Chem.* **2017**, *19*, 4737-4753.
  7. Álvarez-Chávez, C. R.; Edwards, S.; Moure-Eraso, R; Geiser, K. Sustainability of bio-based plastics: General comparative analysis and recommendations for improvement. *J. Clean Prod.* **2012**, *23*, 47–56.
  8. Papageorgiou, G. Z. Thinking Green: Sustainable Polymers from Renewable Resources. *Polymers* **2018**, *10*, 952.
  9. Zhang, Q.; Song, M.; Xu, Y.; Wang, W.; Wang, Z.; Zhang, L. Bio-based polyesters: Recent progress and future prospects. *Prog. Polym. Sci.* **2021**, *120*, 101430.
  10. Morris, A. B. *The Science and Technology of Flexible Packaging. Multilayer Films from Resin and Process to End Use*, Elsevier, **2016**.
  11. Reichert, C. L.; Bugnicourt, E.; Coltelli, M.-B.; Cinelli, P.; Lazzeri, A.; Canesi, I.; Braca, F.; Martínez, B. M.; Alonso, R.; Agostinis, L.; Verstichel, S.; Six, L.; De Mets, S.; Gómez, E. C.; Ißbrücker, C.; Geerinck, R.; Nettleton, D. F.; Campos, I.; Sauter, E.; Pieczyk, P.; Schmid, M. Bio-Based Packaging: Materials, Modifications, Industrial Applications and Sustainability. *Polymers* **2020**, *12*, 1558.
  12. Young, E.; Mirosa, M.; Bremer, P. A Systematic Review of Consumer Perceptions of Smart Packaging Technologies for Food. *Front. Sustain. Food Syst.* **2020**, *4*, 63.

13. Majid, I.; Nayik, G. A.; Dar, S. M.; Nanda, V. Novel food packaging technologies: Innovations and future prospective. *J. Saudi Soc. Agric. Sci.* **2018**, *17*, 454-462.
14. Bhargava, N.; Sharanagat, V. S.; S Mor, R.; Kumar, K. Active and intelligent biodegradable packaging films using food and food waste-derived bioactive compounds: A review. *Trends Food Sci. Technol.* **2020**, *105*, 385-401.
15. Firouz, M. S.; Mohi-Alden, K.; Omid, M. A critical review on intelligent and active packaging in the food industry: Research and development. *Food Res. Int.* **2021**, *141*, 110113.
16. Singh, G.; Singh, S.; Kumar, B.; Gaikwad, K. K. Active barrier chitosan films containing gallic acid based oxygen scavenger. *J. Food Meas. Charact.* **2021**, *15*, 585-593.
17. <https://perfectpackaging.org> (accessed: September 2021).
18. <https://www.flexpack-europe.org> (accessed: September 2021).
19. Vilela, C.; Sousa, A. F.; Fonseca, A. C.; Serra, A. C.; Coelho, J. F. J.; Freire, C. S. R.; Silvestre, A. J. D. The quest for sustainable polyesters – insights into the future. *Polym. Chem.* **2014**, *5*, 3119-3141.
20. Hwang, K. R.; Jeon, W.; Lee, S. Y.; Kim, M. S.; Park, Y. K. Sustainable bioplastics: Recent progress in the production of bio-building blocks for the bio-based next-generation polymer PEF. *Chem. Eng. J.* **2020**, *390*, 124636.
21. Sousa, A. F.; Vilela, C.; Fonseca, A. C.; Matos, M.; Freire, C. S. R.; Gruter, G. J. M.; Coelho, J. F. J.; Silvestre, A. J. D. Biobased polyesters and other polymers from 2,5-furandicarboxylic acid: a tribute to furan excellency. *Polym. Chem.* **2015**, *6*, 5961-5983.
22. Papageorgiou, G. Z.; Papageorgiou, D. G.; Terzopoulou, Z.; Bikiaris, D. N. Production of bio-based 2,5-furan dicarboxylate polyesters: Recent progress and critical aspects in their synthesis and thermal properties. *Eur. Polym. J.* **2016**, *83*, 202-229.
23. Loos, K.; Zhang, R.; Pereira, I.; Agostinho, B.; Hu, H.; Maniar, D.; Sbirrazzuoli, N.; Silvestre, A. J. D.; Guigo, N.; Sousa, A. F. A Perspective on PEF Synthesis, Properties, and End-Life. *Front. Chem.* **2020**, *8*, 585.

24. Terzopoulou, Z.; Papadopoulos, L.; Zamboulis, A.; Papageorgiou, D. G.; Papageorgiou, G. Z.; Bikiaris, D. N. Tuning the Properties of Furandicarboxylic Acid-Based Polyesters with Copolymerization: A Review. *Polymers* **2020**, *12*, 1209.
25. Iglesias, J.; Martínez-Salazar, I.; Maireles-Torres, P.; Martín Alonso, D.; Mariscal, R.; López Granados, M. Advances in catalytic routes for the production of carboxylic acids from biomass: a step forward for sustainable polymers. *Chem. Soc. Rev.* **2020**, *49*, 5704-5771.
26. Chen, C.; Wang, L.; Zhu, B.; Zhou, Z.; El-Hout, S. I.; Yang, J.; Zhang, J. 2,5-Furandicarboxylic acid production via catalytic oxidation of 5-hydroxymethylfurfural: Catalysts, processes and reaction mechanism. *J. Energy Chem.* **2021**, *54*, 528-554.
27. Wojcieszak, R.; Itabaiana, I. Engineering the future: Perspectives in the 2,5-furandicarboxylic acid synthesis. *Catal. Today* **2020**, *354*, 211-217.
28. Dedes, G.; Karnaouri, A.; Topakas, E. Novel Routes in Transformation of Lignocellulosic Biomass to Furan Platform Chemicals: From Pretreatment to Enzyme Catalysis. *Catalysts* **2020**, *10*, 743.
29. Wu, S.; Liu, Q.; Tan, H.; Zhang, F.; Yin, H. A Novel 2,5-Furandicarboxylic Acid Biosynthesis Route from Biomass-Derived 5-Hydroxymethylfurfural Based on the Consecutive Enzyme Reactions. *Appl. Biochem. Biotechnol.* **2020**, *191*, 1470-1482.
30. Naim, W.; Schade, O. R.; Saraci, E.; Wust, D.; Kruse, A.; Grundwaldt, J. D. Toward an Intensified Process of Biomass-Derived Monomers: The Influence of 5-(Hydroxymethyl)furfural Byproducts on the Gold-Catalyzed Synthesis of 2,5-Furandicarboxylic Acid. *ACS Sustainable Chem. Eng.* **2020**, *8*, 11512-11521.
31. Deshan, A. D. K.; Atanda, L.; Moghaddam, L.; Rackemann, D. W.; Beltramini, J.; Doherty, W. O. S. Heterogeneous Catalytic Conversion of Sugars Into 2,5-Furandicarboxylic Acid. *Front. Chem.* **2020**, *8*, 659.
32. Guidotti, G.; Soccio, M.; García-Gutiérrez, M. C.; Gutiérrez-Fernández, E.; Ezquerra, T. A.; Siracusa, V.; Munari, A.; Lotti, N. Evidence of a 2D-Ordered Structure in Biobased

- Poly(pentamethylene furanoate) Responsible for Its Outstanding Barrier and Mechanical Properties. *ACS Sustainable Chem. Eng.* **2019**, 7, 17863–17871.
33. Guidotti, G.; Soccio, M.; García-Gutiérrez, M. C.; Ezquerra, T.; Siracusa, V.; Gutiérrez-Fernández, E.; Munari, A.; Lotti, N. Fully Biobased Superpolymers of 2,5-Furandicarboxylic Acid with Different Functional Properties: From Rigid to Flexible, High Performant Packaging Materials. *ACS Sustainable Chem. Eng.* **2020**, 8, 9558–9568.
34. Benson, N. U.; Bassey D. E.; Palanisami, T. COVID pollution: impact of COVID-19 pandemic on global plastic waste footprint. *Heliyon* **2021**, 7, e06343.
35. Klemeš, J. J.; Van Fan, Y.; Tan, R. R.; Jiang, P. Minimising the present and future plastic waste, energy and environmental footprints related to COVID-19. *Renewable Sustainable Energy Rev.* **2020**, 127, 109883.
36. Khoo, K. S.; Ho, L. Y.; Lim, H. R.; Leong, H. Y.; Chew, K. W. Plastic waste associated with the COVID-19 pandemic: Crisis or opportunity? *J. Hazard. Mater.* **2021**, 417, 126108.
37. Pellis, A.; Haernvall, K.; Pichler, C. M.; Ghazaryan, G.; Breinbauer, R.; Guebitz, G. M. Enzymatic hydrolysis of poly(ethylene furanoate). *J. Biotechnol.* **2016**, 235, 47-53.
38. Gigli, M.; Quartinello, F.; Soccio, M.; Pellis, A.; Lotti, N.; Guebitz, G. M.; Licoccia, S.; Munari, A. Enzymatic hydrolysis of poly(1,4-butylene 2,5-thiophenedicarboxylate) (PBTF) and poly(1,4-butylene 2,5-furandicarboxylate) (PBF) films: A comparison of mechanisms. *Environ. Int.* **2019**, 130, 104852.
39. Okada, M.; Tachikawa, K.; Aoi, K. Biodegradable polymers based on renewable resources. II. Synthesis and biodegradability of polyesters containing furan rings. *J. Polym. Sci., Part A: Polym. Chem.* **1997**, 35, 2729–2737.
40. Muller, R. J.; Kleeberg, I.; Deckwer, W. D. Biodegradation of polyesters containing aromatic constituents. *J. Biotechnol.* **2001**, 86, 87–95.

41. Soccio, M.; Costa, M.; Lotti, N.; Gazzano, M.; Siracusa, V.; Salatelli, E.; Manaresi, P.; Munari, A. Novel fully biobased poly(butylene 2,5-furanoate/diglycolate) copolymers containing ether linkages: Structure-property relationships. *Eur. Polym. J.* **2016**, *81*, 397–412.
42. Guidotti, G.; Soccio, M.; Lotti, N.; Siracusa, V.; Gazzano, M.; Munari, A. New multi-block copolyester of 2,5-furandicarboxylic acid containing PEG-like sequences to form flexible and degradable films for sustainable packaging. *Polym. Degrad. Stab.* **2019**, *169*, 108963.
43. Cowie, J. M. G.; Arrighi, V. *Polymers Chemistry and Physics of Modern Materials*, 3<sup>rd</sup> Edition, CRC Press, **2007**, Chapter 15.
44. Pouloupoulou, N.; Smyrnioti, D.; Nikolaidis, G. N.; Tsitsimaka, I.; Christodoulou, E.; Bikiaris, D. N.; Charitopoulou, M. A.; Achilias, D. S.; Kapnisti, M.; Papageorgiou, G. Z. Sustainable Plastics from Biomass: Blends of Polyesters Based on 2,5-Furandicarboxylic Acid. *Polymers* **2020**, *12*, 225.
45. Thiyagarajan, S.; Vogelzang, W.; Knoop, R. J. I.; Frissen, A. E.; van Haveren, J.; van Es, D. S. Biobased furandicarboxylic acids (FDCAs): effects of isomeric substitution on polyester synthesis and properties. *Green Chem.* **2014**, *16*, 1957-1966.
46. Soccio, M.; Nogales, A.; García-Gutiérrez, M.; Lotti, N.; Munari, A.; Ezquerra, T. Origin of the subglass dynamics in aromatic polyesters by labeling the dielectric relaxation with ethero atoms. *Macromolecules* **2008**, *41*, 2651–2655.
47. Bianchi, E.; Soccio, M.; Siracusa, V.; Gazzano, M.; Thiyagarajan, S.; Lotti, N. Poly(butylene 2,4-furanoate), an Added Member to the Class of Smart Furan-Based Polyesters for Sustainable Packaging: Structural Isomerism as a Key to Tune the Final Properties. *ACS Sustainable Chem. Eng.* **2021**, *9*, 11937–11949.
48. Thiyagarajan, S.; Meijlink, M. A.; Bourdet, A.; Vogelzang, W.; Knoop, R. J. I.; Esposito, A.; Dargent, E.; van Es, D. S.; van Haveren, J. Synthesis and Thermal Properties of Bio-Based Copolyesters from the Mixtures of 2,5- and 2,4-Furandicarboxylic Acid with Different Diols. *ACS Sustainable Chem. Eng.* **2019**, *7*, 18505–18516.



49. Nolasco, M. M.; Araujo, C. F.; Thiagarajan, S.; Rudić, S.; Vaz, P. D.; Silvestre, A. J. D.; Ribeiro-Claro, P. J. A.; Sousa, A. F. Asymmetric Monomer, Amorphous Polymer? Structure–Property Relationships in 2,4-FDCA and 2,4-PEF. *Macromolecules* **2020**, *53*, 1380–1387.
50. Robertson, G. L. *Food Packaging Principles and Practice*, 3<sup>rd</sup> Edition, CRC Press, **2013**, Chapter 2-4.
51. Davidson, M. G.; Elgie, S.; Parsons, S.; Young, T. J. Production of HMF, FDCA and their derived products: a review of life cycle assessment (LCA) and techno-economic analysis (TEA) studies. *Green Chem.* **2021**, *23*, 3154-3171.
52. Bozell, J. J.; Petersen, G. R. Technology development for the production of biobased products from biorefinery carbohydrates—the US Department of Energy’s “Top 10” revisited. *Green Chem.* **2010**, *12*, 539-554.
53. Bio-Based Chemicals A 2020 Update, IEA Bioenergy, available online: <https://www.ieabioenergy.com/wp-content/uploads/2020/02/Bio-based-chemicals-a-2020-update-final-200213.pdf> (accessed September 2021).
54. Zheng, M.; Li, X. Y.; Guan, R. Q.; Liu, Y. M.; Zhao, Y. J.; Tai, Y. L. Ionic Liquid-Catalyzed Synthesis of Diethylene Glycol. *Adv. Mat. Res.* **2012**, *549*, 287-291.
55. Bioplastics market data, European-bioplastics.org (accessed September 2021).
56. Soccio, M.; Lotti, N.; Finelli, L.; Gazzano, M.; Munari, A. Influence of transesterification reactions on the miscibility and thermal properties of poly(butylene/diethylene succinate) copolymers. *Eur. Polym. J.* **2008**, *44*, 1722-1732.
57. Soccio, M.; Lotti, N.; Gigli, M.; Finelli, L.; Gazzano, M.; Munari, A. Reactive blending of poly(butylene succinate) and poly(triethylene succinate): characterization of the copolymers obtained. *Polym. Int.* **2012**, *61*, 1163-1169.
58. Fabbri, M.; Gigli, M.; Gamberini, R.; Lotti, N.; Gazzano, M.; Rimini, B.; Munari, A. Hydrolysable PBS-based poly(ester urethane)s thermoplastic elastomers. *Polym. Degrad. Stab.* **2014**, *108*, 223-231.

59. Lotti, N.; Finelli, L.; Fiorini, M.; Righetti, M. C.; Munari, A. Synthesis and characterization of poly(butylene terephthalate-co-diethylene terephthalate) copolyesters. *Polymer* **2000**, *41*, 5297-5304.
60. Lotti, N.; Finelli, L.; Fiorini, M.; Righetti, M. C.; Munari, A. Synthesis and characterization of poly(butylene terephthalate-co-triethylene terephthalate) copolyesters. *J. Appl. Polym. Sci.* **2001**, *81*, 981-990.
61. Gigli, M.; Lotti, N.; Gazzano, M.; Finelli, L.; Munari, A. Novel eco-friendly random copolyesters of poly(butylene succinate) containing ether-linkages. *React. Funct. Polym.* **2012**, *72*, 303-310.
62. Gigli, M.; Lotti, N.; Gazzano, M.; Siracusa, V.; Finelli, L.; Munari, A.; Dalla Rosa, M. Fully aliphatic copolyesters based on poly(butylene 1,4-cyclohexanedicarboxylate) with promising mechanical and barrier properties for food packaging applications. *Ind. Eng. Chem. Res.* **2013**, *52*, 12876–12886.
63. Gigli, M.; Lotti, N.; Gazzano, M.; Siracusa, V.; Finelli, L.; Munari, A.; Dalla Rosa, M. Biodegradable aliphatic copolyesters containing PEG-like sequences for sustainable food packaging applications. *Polym. Degrad. Stab.* **2014**, *105*, 96-106.
64. Kainulainen, T. P.; Hukka, T. I.; Ozeren, H. D.; Sirvio, J. A.; Hedenqvist, M. S.; Heiskanen, J. P. Utilizing Furfural-Based Bifuran Diester as Monomer and Comonomer for High-Performance Bioplastics: Properties of Poly(butylene furanoate), Poly(butylene bifuranoate), and Their Copolyesters. *Biomacromolecules* **2020**, *21*, 743–752.
65. Jiang, Y.; Woortman, A. J. J.; Alberda van Ekensteina, G. O. R.; Loos, K. A biocatalytic approach towards sustainable furanic–aliphatic polyesters. *Polym. Chem.* **2015**, *6*, 5198-5211.
66. Haernvall, K.; Zitzenbacher, S.; Amer, H.; Zumstein, M. T.; Sander, M.; McNeill, K.; Yamamoto, M.; Schick, M. B.; Ribitsch, D.; Guebitz, G. M. Polyol Structure Influences Enzymatic Hydrolysis of Bio-Based 2,5-Furandicarboxylic Acid (FDCA) Polyesters. *Biotechnol. J.* **2017**, *12*, 1600741.

67. Papageorgiou, G. Z.; Papageorgiou, D. G.; Terzopoulou, Z.; Bikiaris, D. N. Production of bio-based 2,5-furan dicarboxylate polyesters: Recent progress and critical aspects in their synthesis and thermal properties. *Eur. Polym. J.* **2016**, *83*, 202-229.
68. Tsanaktsis, V.; Terzopoulou, Z.; Nerantzaki, M.; Papageorgiou, G. Z.; Bikiaris, D. N. New poly(pentylene furanoate) and poly(heptylene furanoate) sustainable polyesters from diols with odd methylene groups. *Mater. Lett.* **2016**, *178*, 64-67.
69. Diao, L.; Su, K.; Li, Z.; Ding, C. Furan-based co-polyesters with enhanced thermal properties: poly(1,4-butylene-co-1,4-cyclohexanedimethylene-2,5-furandicarboxylic acid) [\*RSC Adv.\*](#) **2016**, *6*, 27632-27639.
70. Cottrell, T. L. *The Strengths of Chemical Bonds*, Butterworths, 2<sup>nd</sup> ed., London, 1958.
71. Martinez-Tong, D. E.; Soccio, M.; Robles-Hernández, B.; Guidotti, G.; Gazzano, M.; Lotti, N.; Alegria, A. Evidence of Nanostructure Development from the Molecular Dynamics of Poly(pentamethylene 2,5-furanoate). *Macromolecules* **2020**, *53*, 10526-10537.
72. Araujo, C. F.; Nolasco, M. M.; Ribeiro-Claro, P. J. A.; Rudic, S.; Silvestre, A. J. D.; Vaz, P. D.; Sousa, A. F. Inside PEF: chain conformation and dynamics in crystalline and amorphous domains. *Macromolecules* **2018**, *51*, 3515–3526.
73. Patkar, M.; Jabarin, S. A. Effect of diethylene glycol (DEG) on the crystallization behavior of poly(ethylene terephthalate) (PET). *J. Appl. Polym. Sci.* **1993**, *47*, 1749-1763.
74. Soccio, M.; Lotti, N.; Finelli, L.; Gazzano, M.; Munari, A. Aliphatic poly(propylene dicarboxylate)s: Effect of chain length on thermal properties and crystallization kinetics. *Polymer* **2007**, *48*, 3125-3136.
75. Liang, H.; Hao, Y.; Liu, S.; Zhang, H.; Li, Y.; Dong, L.; Zhang, H. Thermal, rheological, and mechanical properties of polylactide/poly(diethylene glycol adipate). *Polym. Bull.* **2013**, *70*, 3487–3500.
76. Cao, A.; Okamura, T.; Nakayama, K.; Inoue, Y.; Masuda, T. Studies on syntheses and physical properties of biodegradable aliphatic poly(butylene succinate-co-ethylene

- succinate)s and poly(butylene succinate-co-diethylene glycol succinate)s. *Polym. Degrad. Stab.* **2002**, *78*, 107-117.
77. Zeng, J. B.; Huang, C. L.; Jiao, L.; Lu, X.; Wang, Y. Z.; Wang, X. L. Synthesis and Properties of Biodegradable Poly(butylene succinate-co-diethylene glycol succinate) Copolymers. *Ind. Eng. Chem. Res.* **2012**, *51*, 12258–12265.
78. Rudyak, V. Y.; Gavrilov, A. A.; Guseva, D. V.; Tung, S. H.; Komarov, P. V. Accounting for  $\pi$ - $\pi$  stacking interactions in the mesoscopic models of conjugated polymers. *Mol. Syst. Des. Eng.* **2020**, *5*, 1137.
79. Sago, T.; Itagaki, H.; Asano, T. Onset of Forming Ordering in Uniaxially Stretched Poly(ethylene terephthalate) Films Due to  $\pi$ - $\pi$  Interaction Clarified by the Fluorescence. *Macromolecules* **2014**, *47*, 217–226.
80. Shanavas, A.; Sathiyaraj, S.; Chandramohan, A.; Narasimhaswamy, T.; Sultan Nasar, A. Isophthalic acid based mesogenic dimers: Synthesis and structural effects on mesophase properties. *J. Mol. Struct.* **2013**, *1038*, 126-133.
81. Mahendrasingam, A.; Blundell, D. J.; Martin, C.; Urban, V.; Narayanan, T.; Fuller, W. Time resolved WAXS study of the role of mesophase in oriented crystallisation of poly(ethylene terephthalate-co-isophthalate) copolymers. *Polymer* **2005**, *46*, 6044-6049.
82. Nolasco, M. M.; Araujo, C. F.; Thiyagarajan, S.; Rudić, S.; Vaz, P. D.; Silvestre, A. J. D.; Ribeiro-Claro, P. J. A.; Sousa, A. F. Asymmetric Monomer, Amorphous Polymer? Structure–Property Relationships in 2,4-FDCA and 2,4-PEF. *Macromolecules* **2020**, *53*, 1380–1387.
83. (Burgess, S. K.; Leisen J. E.; Kraftschik, B. E.; Mubarak, C. R., Kriegel, R. M.; Koros, W. J. Chain Mobility, Thermal, and Mechanical Properties of Poly(ethylene furanoate) Compared to Poly(ethylene terephthalate). *Macromolecules* **2014**, *47*, 1383–1391.
84. Bourdet, A.; Esposito, A.; Thiyagarajan, S.; Delbreilh, L.; Affouard, F.; Knoop, R. J. I.; Dargent, E. Molecular Mobility in Amorphous Biobased Poly(ethylene 2,5-

furandicarboxylate) and Poly(ethylene 2,4-furandicarboxylate). *Macromolecules* **2018**, *51*, 1937–1945.

85. Hedenqvist, M. S. Barrier Packaging Materials, in: Kutz, M. (Ed.), *Handbook of Environmental Degradation of Materials*, Elsevier Inc., 2<sup>nd</sup> ed., **2012**, pp. 833–860.

86. Burgess, S. K.; Kriegel, R. M.; Koros, W. J. Carbon dioxide sorption and transport in amorphous poly (ethylene furanoate). *Macromolecules* **2015**, *48*, 2184–2193.

87. Guidotti, G.; Genovese, L.; Soccio, M.; Gigli, M.; Munari, A.; Siracusa, V.; Lotti, N. Block Copolyesters Containing 2,5-Furan and trans-1,4-Cyclohexane Subunits with Outstanding Gas Barrier Properties. *Int. J. Mol. Sci.* **2019**, *20*, 1–15.

88. Guidotti, G.; Soccio, M.; Lotti, N.; Gazzano, M.; Siracusa, V.; Munari, A. Poly (propylene 2, 5-thiophenedicarboxylate) vs. Poly (propylene 2, 5-furandicarboxylate): Two examples of high gas barrier bio-based polyesters. *Polymers* **2018**, *10*, 785.

89. Guidotti, G.; Gigli, M.; Soccio, M.; Lotti, N.; Gazzano, M.; Siracusa, V.; Munari, A. Ordered structures of poly (butylene 2, 5-thiophenedicarboxylate) and their impact on material functional properties. *Eur. Polym. J.* **2018**, *106*, 284–290.